Neural Representation for Color-selective Populations in the Pigeon Entopallium

Authors: Qingzhi He[1], Juncai Zhu[1], Xiaoke Niu[1], Peng Wu[1], Rupeng Zhang[1], Bo Li[1], Jiangtao Wang[1]*, Zhizhong Wang[1]*

[1] School of Electrical and Information Engineering, Zhengzhou University, Zhengzhou, Henan 450001, China

ABSTRACT

Understanding how birds encode object color is fundamental to elucidating the neural mechanisms of color vision. Although behavioral studies have demonstrated high color discrimination accuracy in birds, it remains unclear whether higher-order visual areas structurally encode color information. Here, we performed multi-site multi-unit activity recordings from the pigeon entopallium while presenting multi-category images that systematically varied in hue, luminance, and saturation. Numerous entopallium sites exhibited robust hue selectivity that remained stable across luminance and saturation changes, with population responses primarily gain modulation. Simultaneously, these sites demonstrated category-invariant color selectivity within the tested object set. Population-level analyses revealed a distinct and structured representational geometry that corresponded closely to perceptual color axes, with color-related correlations markedly stronger than category-related correlations. These results suggest that the pigeon entopallium exhibits population-level color

coding, yielding a hue-related representational geometry that is broadly consistent with reports from primate V4 under comparable stimulus manipulations.

Keywords: Pigeon; Entopallium; Hue selectivity; Neural coding; Color representation.

INTRODUCTION

Birds possess a highly developed visual system and exhibit exceptional color discrimination, which plays a crucial role in object recognition, predator avoidance, mate choice, and social signaling (Burley and Coopersmith, 2010; Collins et al., 1994; Zeigier and Bischoff, 1994). This remarkable ability arises from the presence of four types of wavelength-sensitive cone photoreceptors and associated pigmented oil droplets in the avian retina (Bowmaker et al., 1997; Chen and Goldsmith, 1986; Kelber, 2019), providing broader spectral sampling and finer chromatic resolution compared with the trichromatic system of most mammals(Hart and Vorobyev, 2005; Kelber et al., 2003). Although color perception originates from differential activation among cone types, it remains unclear how avian higher visual areas integrate and represent color information at the cortical level. Color is determined by hue(H), saturation(S) and luminance(L) (Conway, 2009; Endler et al., 2005; Price et al., 2019), and understanding how these dimensions are organized in the avian brain is critical for revealing the neural principles of color coding. Importantly, color representation involves not only local chromatic extraction but also integration with spatial, shape, and texture information to achieve stable recognition and adaptive behavioral responses (Bennett and Cuthill, 1994; Chang et al., 2017). Exploring the neural mechanisms of color representation and feature integration in the avian

higher visual system is therefore essential for understanding the foundations of avian visual cognition.

In the avian visual system, retinal signals reach higher visual areas through two major ascending pathways, commonly referred to as the thalamofugal and tectofugal pathways (Niu et al., 2022; Pusch et al., 2023; Straight et al., 2024). The thalamofugal pathway relays information from the retina via the dorsal lateral geniculate nucleus to the Wulst, where it has been linked primarily to spatial vision and pattern analysis. By contrast, the tectofugal pathway transmits visual signals through the optic tectum and associated thalamic nuclei to the entopallium, and is thought to play a central role in the processing of complex visual features such as color, shape, and motion (Hsiao et al., 2020). In line with this anatomical organization, a range of behavioral and electrophysiological studies have highlighted the entopallium as a key region for color and shape related processing and feature integration in birds (Collins et al., 1994; Cook, 2013; Hsiao et al., 2020; Jarvis et al., 2005; Wang et al., 2025). Research on avian color perception has so far focused on two main directions. First, behavioral studies have shown that focal lesions of the entopallium markedly impair performance in color discrimination tasks, suggesting its essential contribution to color-related visual cognition (Cook, 2013; Watanabe et al., 2008). Second, electrophysiological evidence indicates that under fixed luminance and saturation conditions, some neurons in the zebra finch entopallium exhibit selective responses to particular hues, with the strongest activity elicited by blue stimuli (Hsiao et al., 2020; Stacho et al., 2016). However, most studies have used simplified color-discrimination tasks or varied only one dimension of color space, leaving the integrative coding of hue, luminance and saturation in the avian entopallium largely uncharacterized.

In contrast, studies in primates have achieved more substantial progress in elucidating the neural mechanisms of color representation. Extensive evidence indicates that color-selective neurons are distributed across multiple cortical areas, with some maintaining stable hue tuning across different object categories(Conway et al., 2007; Xiao et al., 2003), whereas others exhibit hue preferences that vary with object identity. Moreover, several studies have reported neurons showing strong selectivity for a narrow range of hues (Johnson et al., 2001; Komatsu et al., 1992). These findings suggest the presence of adjacent but functionally specialized cortical subregions in the primate brain, responsible for encoding color, object category, and their interactions. Research on avian visual systems remains limited in systematic analyses of single-site and population coding across multiple object categories. In particular, little is known about how color information is organized in representational space or how effectively it supports color decoding in higher visual areas. It also remains unclear whether neurons in the entopallium maintain stable hue tuning across categories and whether population activity forms structured representations that enable reliable color decoding. Clarifying these questions will advance understanding of hierarchical color processing and the integration of color and object representations in the avian brain.

To elucidate the neural mechanisms underlying color processing in the avian visual system, we investigated pigeons using a color-category orthogonal stimulus set. We investigated whether the geometry of the neural representational space is systematically modulated by luminance and saturation and whether such modulation conforms to perceptual organization in color space. We then tested whether hue tuning is preserved across object categories. Finally, we asked whether population activity dissociates chromatic from categorical structure and

quantified the relative contributions of color- and category-related information to the population code. This study provides empirical evidence for multidimensional color representations in the avian brain and characterizes population-level color coding in a higher visual area. Our results can be discussed in relation to primate V4 and other color-processing circuits, facilitating cross-species comparisons at the level of population representational geometry under the tested stimulus conditions.

MATERIALS AND METHODS

Subjects

Fourteen adult pigeons (*Columba livia*; body weight 350-400 g) were used in this study. All subjects were housed individually in stainless-steel cages maintained at 20 ± 2 °C under a 12 h light/dark cycle (lights on at 08:00 and off at 20:00). Body weight was controlled at 80-85% of the level by regulating a mixed-grain diet, and water was available. All experimental procedures conformed to the guidelines of the National Institutes of Health (NIH, USA) for the care and use of laboratory animals and strictly complied with the Regulations on the Administration of Laboratory Animals of the People's Republic of China. The study protocol was reviewed and approved by the Ethics Committee for Animal Research at Zhengzhou University.

Surgery

Pigeons were anesthetized with urethane (20% w/v, 1.0 ml/100 g, i.p.), chosen for its ability to maintain exceptional physiological stability and consistent anesthetic depth throughout the

multi-hour recording sessions without the need for supplementation (Xiao and Frost, 2009). The subjects were secured in a stereotaxic frame (RWD Life Science Co., Ltd., Shenzhen, China). Following a midline scalp incision, a small craniotomy was performed to expose the brain surface. Stereotaxic coordinates for the left entopallium were determined according to the pigeon brain atlas (Krützfeldt and Wild, 2005): AP 9.5-10.5 mm, ML 5.0-6.0 mm (Appendix Figure A3). Neural signals were recorded using a 32-channel tungsten microelectrode array (4 × 8 grid of 32 independent electrodes; 350 μm spacing in both row and column directions; 7 mm shank length; 800 kΩ impedance; KEDOU Neurotech Co., Ltd., Suzhou, China). After the dura was reflected with a fine needle, the array was slowly advanced to the target depth (DV 4.0-5.0 mm; Appendix Figure A3). The reference wire was inserted subcutaneously with the pial surface serving as the zero-depth reference. To ensure stable monocular stimulation, the left eye was occluded, and the right eyelid was surgically removed. All recordings were conducted under anesthesia with the head rigidly fixed. Upon completion of the session, pigeons were euthanized via an intraperitoneal overdose of urethane (1.5 ml/100 g), in accordance with local and national ethical guidelines for animal research.

Neural Signal Recording

Neural signals were acquired, amplified, filtered, and digitized using a Cerebus multichannel recording system (Blackrock Microsystems, Salt Lake City, UT, USA) at a sampling rate of 30 kHz. The raw signals were band-pass filtered 250-5kHz, and neuronal spiking events were detected by threshold crossing, with thresholds set at −4 to −6 times the standard deviation of the background noise. The extracted spike trains were not subjected to single-unit isolation but

were analyzed as multi-unit activity sites (MUA), representing the aggregate firing of neuronal populations in the vicinity of each recording electrode. MUA was used as a population-level readout of local neuronal activity, providing a stable and reproducible measure of collective firing dynamics without requiring spike sorting. This approach allowed us to quantify the overall responsiveness and discriminability of local neuronal ensembles under different stimulus conditions. Each recording session lasted approximately 3.5 hours under anesthesia with the head fixed in the stereotaxic apparatus. Under these conditions, voluntary eye movements were absent, and online eye position tracking was therefore not required. Task-related events (e.g., stimulus onset and offset) were recorded as transistor-transistor logic (TTL) pulses and time-locked to the neural data to ensure precise temporal alignment for subsequent analyses (Appendix FigureA1).

Visual Stimulation Presentation

A series of visual stimuli were presented to probe the color responsiveness of neurons. All stimulus paradigms were generated in MATLAB using the Psychtoolbox (PTB). Stimuli were displayed on a 50-inch OLED monitor (AOC AG485UD, 16:9 aspect ratio) positioned 20–40 cm in front of the pigeon's head. The monitor had a resolution of 3840 × 2160 pixels and a refresh rate of 100 Hz, with a pixel density of 36.486 pixels/cm. Under this setup, the display provided a maximum visual field coverage of approximately 138° × 112° at the closest viewing distance. The viewing distance was allowed to vary within 20–40 cm to ensure that the stimuli consistently covered the receptive-field region of neurons in the entopallium mapped for each subject, thereby maintaining effective stimulation of the recorded sites across trials. Because

the visual axis of one pigeon eye forms an angle of 61° with the beak-tail axis, the stereotaxic frame was rotated by 29° to align the monitor with the frontal visual field. The line connecting the beak tip and the center of the eye normally forms an angle of 34° with the horizontal plane, which increased to 72° when the bird was fixed in the stereotaxic apparatus. To compensate for this change, the monitor was tilted by 38° to match the natural viewing direction. Under urethane anesthesia with rigid head fixation, stimulus placement was controlled based on receptive field mapping. Before the main color experiments, we mapped the classical receptive field for each recording site using a position-sampling procedure (small stimuli were flashed at pseudorandom locations on a predefined screen grid, and a position-by-position response map was computed from the mean evoked activity; see Appendix for full details). All stimuli in the main experiment were then presented within the mapped receptive field region.

Construction of Stimulus Set

A total of 225 visual stimuli were designed, consisting of five natural object categories (cup, food, pigeon, Rubik's cube, and watermelon). For each category, stimuli were generated from 8 hue conditions sampled every 45° along the color wheel (1°-360°) and 5 luminance-saturation (L-S) combinations, and additionally included a luminance-matched grayscale control condition for each L-S combination. Thus, the dataset comprised 200 color images (5 categories × 8 hues × 5 L-S combinations) and 25 grayscale images (5 categories ×5 L-S combinations). Stimuli were generated in MATLAB using Psychtoolbox and displayed on a γ-corrected monitor ($\gamma \approx 2.2$) calibrated for chromaticity and luminance (maximum luminance: 300 cd/m²). Hue values were sampled every 45° along the color wheel (1°-360°), and grayscale

images were mapped to hue channels to produce eight colored versions plus one luminance-matched grayscale condition. Luminance was set to three levels (L1=50 cd/m², L2=150 cd/m², L3=200 cd/m²) and saturation to three levels (S1=0.5, S2=0.8, S3=1.0). Five luminance-saturation combinations (S1-L2, S2-L2, S3-L2, S3-L3 and S3-L1) formed a full factorial design across hue, luminance and saturation for assessing neuronal tuning in three color dimensions. All stimuli were centered on the receptive field, scaled to cover the main area, and presented on a neutral gray background for 500ms. Each trial was followed by an 18s gray interval to minimize adaptation. All color and grayscale stimuli were pooled into a single stimulus list and presented in a pseudorandom order; the full sequence was repeated three times, with the stimulus order randomized independently for each repetition.

Data analysis

Selection of color-selective sites: Visually responsive channels were first identified by applying an activity threshold, excluding those with mean peak firing rates below 30 spikes/s. The mean firing rate was calculated between 100 and 300ms after stimulus onset to compare responses to color and luminance-matched grayscale stimuli. A site was classified as color-selective if its maximum response to a color stimulus was at least twice that to the corresponding grayscale image. Furthermore, for each stimulus set and repetition, responses to the same color were averaged across the five object categories to obtain the overall color response. One-way ANOVA was performed to assess differences among the eight hue conditions ($p < 0.001$). Only sites showing significant color tuning were included in subsequent representational analyses.

Population Representational Geometry and Multidimensional Scaling: Neural responses were quantified as spike counts within a 50-350ms window after stimulus onset. Responses of all sites across stimulus conditions were z-scored to achieve 0 mean and 1 variance. For analyses focusing on the neural representation of a single feature (color), responses were averaged across the irrelevant feature dimension (category). Classical multidimensional scaling was then performed on population response patterns using Euclidean distance and MATLAB's cmdscale function. For each site, responses were normalized to zero mean and unit variance. The Euclidean distance between population responses to two stimulus conditions was computed to quantify their neural distance. Based on the same normalized population response, the similarity matrix of correlation coefficients was computed between the population response vectors (across all color-selective sites, averaged over stimulus repeats) to each of the n interested conditions.

Population statistics: To evaluate the statistical significance of population-level estimates (e.g., correlation coefficients), a bootstrap resampling procedure was used. Neurons were randomly resampled with replacement from the original population to generate bootstrap samples of equal size, repeated 20,000 times. The target statistic was computed for each iteration to form an empirical distribution, and p-values were obtained by comparing the observed value with this distribution under the null hypothesis.

Decoding analysis: We decoded hue information employing supervised support vector (SVM) machine classifiers following established procedures (Haynes, 2009; Hung et al., 2005). Trials were permuted with a fixed seed (rng = 42) and split into 70% training and 30% held-out testing. For each trial, features were the mean firing rates across recording sites in the 50-

300ms post-stimulus window. Neighborhood component analysis was performed on the training set only to rank features; the top 70% were retained and applied unchanged to the test set. Multi-class classification used an error-correcting output codes one-vs-rest scheme with a radial basis function kernel support vector machine (regularization parameter C=5, kernel scale set to auto, feature standardization enabled). Accuracy was computed on the held-out test set; class-wise accuracies were also computed for visualization.

RESULTS

To investigate how neurons in the pigeon entopallium encode object color and category (shape), we designed a stimulus set comprising 45 color stimuli ((8 hues +1 gray) × 5 luminance-saturation combinations) across five object categories (cup, food, pigeon, cube, and watermelon). The stimulus set included 9 hue conditions, consisting of one gray-scale and eight colored image conditions (All the stimulus materials are shown in Figure 1). During data recordings, gray backgrounds alternated with color stimuli; the entire stimulus set was presented three times in randomized order. Neuronal responses typically occurred within 50-300ms after stimulus onset (Appendix Figure A1, raster plots), defining the response window for subsequent analyses. Spike density functions were computed with a 1ms step using a 100ms sliding window (Appendix Figure A1).

Fourteen acute electrophysiological recordings yielded 392 MUA sites in the pigeon entopallium. Based on predefined criteria (see Methods), the mean firing rate within the response window was calculated and averaged across sessions, resulting in 57.4% of sites (225/392) identified as stimulus-responsive. One-way ANOVA further showed that 76.8% of

these sites (173/225) exhibited significant differences in firing rates across eight hue conditions under at least one luminance-saturation combination ($p < 0.001$), and were therefore defined as color-selective sites (Appendix Figure A2). Subsequent analyses of tuning characteristics, representational geometry, and decoding performance were based on this hue-selective population.

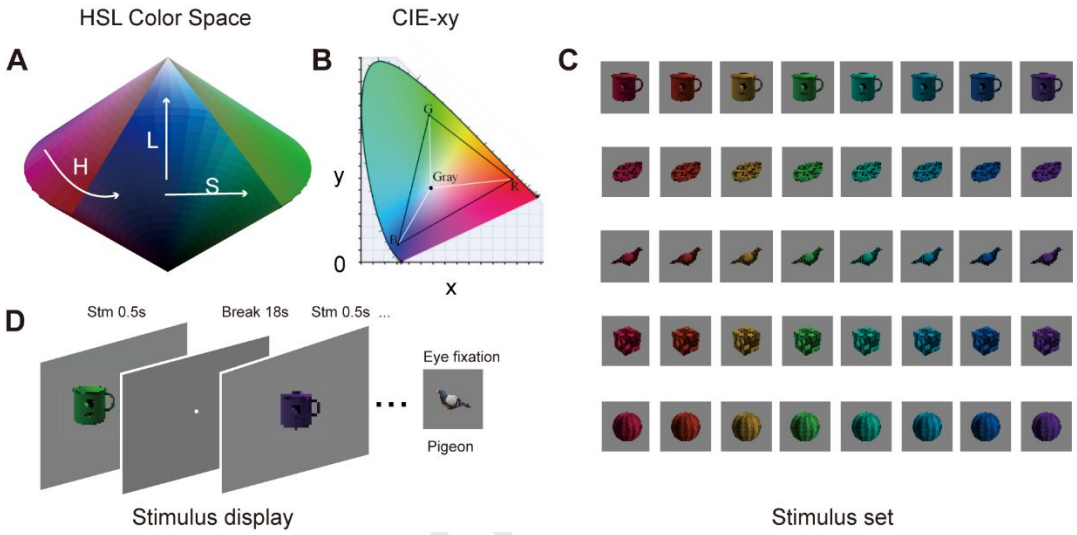

Figure 1 HSL color space and generation of the image stimulus set

A: HSL color space. In this representation, hue rotates around the conical surface from 0° to 360°, saturation increases radially from the center to the edge, and luminance varies vertically from the bottom to the top. B: The spectral output of the display device plotted in CIE-xy chromaticity coordinates. C: The 5 categories used in the experiments. Each image underwent a series of hue-rotation transformations: for a fixed luminance and saturation, the hue coordinates were redistributed along the circumference at the same radial distance as the original image. Eight hue values were selected (starting at 0° and sampled every 45° clockwise), together with three saturation levels (S1, S2, S3) and three luminance levels (L1, L2, L3). These manipulations yielded five luminance-saturation combinations for each hue (S1-L2, S2-L2, S3-L2, S3-L1, and S3-L3), corresponding to conditions with fixed saturation and varying luminance, and fixed luminance with varying saturation. D: The pigeon maintained a fixed viewing position during stimulus presentation.

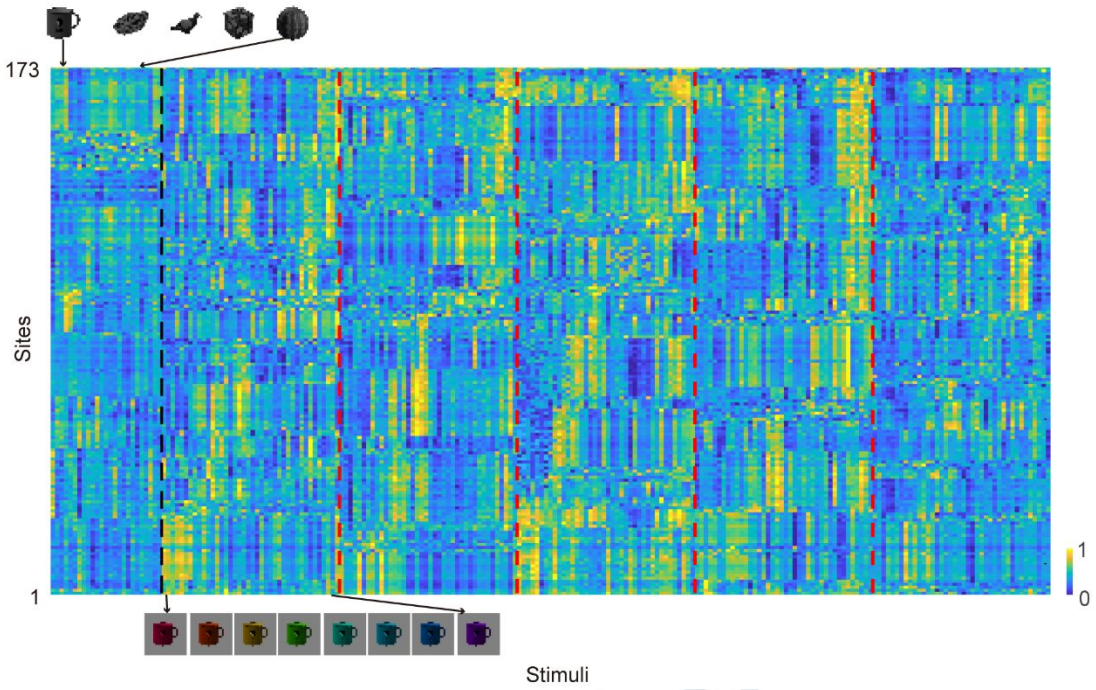

Figure 2 Responses of color-selective sites to gray and color stimuli

Average responses of color-selective sites were aligned according to preferred hue. Each row represents a single MUA site, and the horizontal axis indexes stimulus conditions (object category × hue level, including grayscale). Baseline activity was removed, and responses were normalized to z-scores. Sites from all 14 recording sessions were pooled and sorted by preferred hue (not grouped by session).

After sorting by hue preference, population responses were visualized as a response matrix (Figure 2). Under grayscale conditions, neuronal activity exhibited no apparent structure and appeared largely random. In contrast, color stimuli elicited a continuous and orderly gradient of responses across the neuronal population. Dashed lines mark the boundaries between the tested object categories, the hue-related response structure did not exhibit systematic discontinuities at these boundaries. Together, these results indicate that, within the specific range of object categories and physical similarities tested here, color representations in the entopallium are dominated by a continuous coding of hue across object contexts (Chang et al., 2017; Xiao et al., 2007).

Color tuning characteristics of color-selective sites

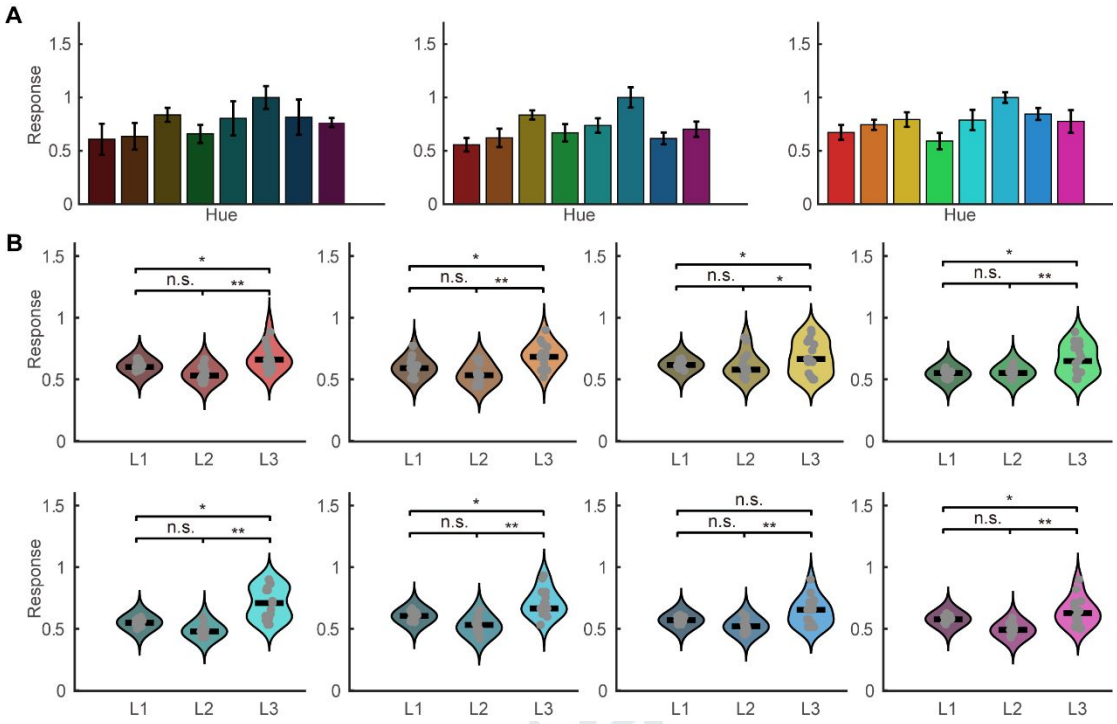

Figure 3 Response characteristics of an example color-selective MUA site under different luminance conditions

A: Mean firing rates of an example color-selective MUA site in response to eight hue stimuli under three luminance levels (L1, L2, L3). For each hue and luminance level, responses were first averaged across repeated trials and then averaged across object categories. Error bars indicate the standard error of the mean (SEM) across object categories. B: Distribution of responses across three luminance conditions (L1, L2, L3). Violin plots with overlaid data points (15 points) are used to show the response distribution, with pairwise statistical comparisons shown above the plots (n.s., not significant; *: $p < 0.05$; **: $p < 0.01$).

Sites in entopallium exhibited orderly and stable hue preferences across luminance conditions. As shown in Figure 3A, from left to right are neural response distributions under low (L1), medium (L2), and high (L3) luminance levels. The representative site displayed a consistent preference for blue (H6) across all three luminance conditions, indicating that changes in luminance did not alter its hue selectivity. Rank-order analysis further confirmed the robustness of hue tuning, yielding an Order Similarity Index (OSI) of 0.76 and Kendall's

coefficient of concordance (W) of 0.83. Statistical comparisons of the response distributions revealed stronger at L3，differing significantly from those at L1 and L2, whereas L1 and L2 did not differ significantly (Figure 3B), following a modulation trend of L2 < L1< L3. Collectively, these findings indicate that hue preference remains highly stable across luminance changes, while luminance exerts a consistent, gain modulation on response strength(Hermann et al., 2022).

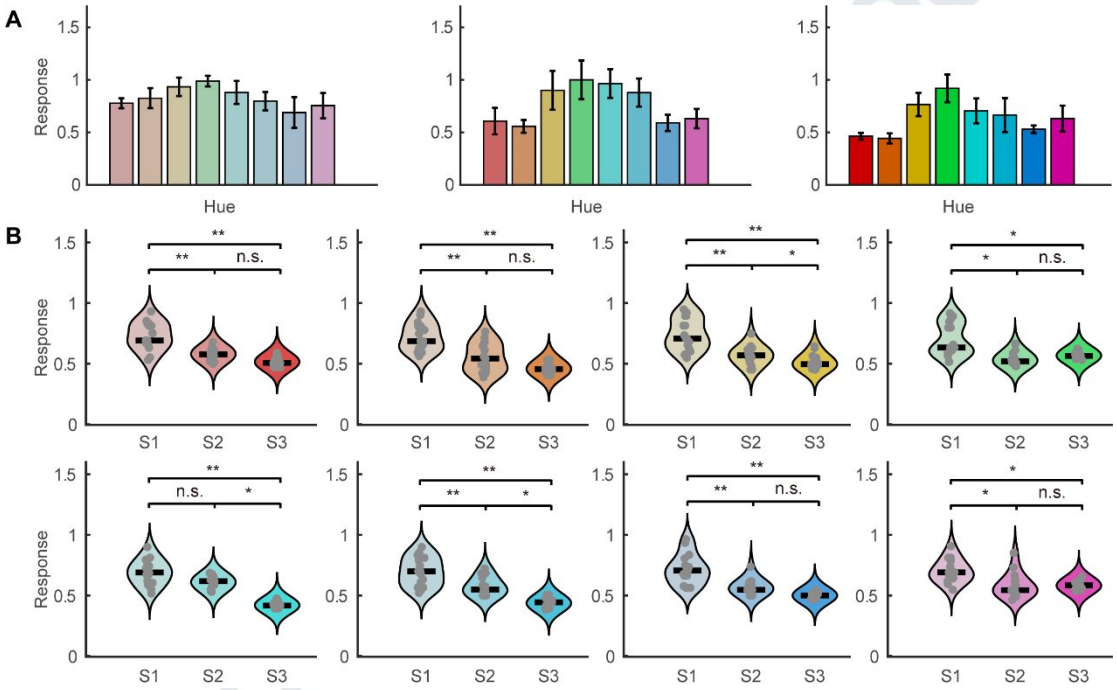

Figure 4 Response characteristics of an example color-selective MUA site under different saturation conditions

A: Mean firing rates of an example color-selective MUA site in response to eight hue stimuli across different saturation levels (S1, S2, S3). For each hue and saturation level, responses were first averaged across repeated trials and then averaged across object categories. Error bars indicate the standard error of the mean (SEM) across object categories. B: Distribution of responses across three saturation conditions (S1, S2, S3). Violin plots with overlaid data points (15 points) are used to show the response distribution, with pairwise statistical comparisons shown above the plots (n.s., not significant; *: $p < 0.05$; **: $p < 0.01$).

After confirming that luminance modulates hue tuning through gain modulation, we examined how saturation affects hue selectivity. As shown in Figure 4A, the responses under

low (S1), medium (S2), and high (S3) saturation conditions are presented from left to right. The site consistently preferred green (H4) across all saturation levels, indicating that saturation changes did not affect hue selectivity(Stoughton and Conway, 2008). Rank-order analysis further demonstrated strong consistency of hue tuning, yielding an Order Similarity Index (OSI) of 0.80 and Kendall's coefficient of concordance (W) of 0.89. Statistical comparisons of the response distributions showed that responses at S1 were significantly stronger than those at S2 and S3, while no significant difference was found between S2 and S3 (Figure 4B), following a modulation trend of S1 > S2 > S3. These results indicate that hue preference remains robust across saturation changes, with saturation mainly influencing response strength rather than the hue selectivity (Bohon et al., 2016).

Together, these findings demonstrate that across variations in luminance and saturation, color-selective sites exhibit changes mainly in response gain rather than in hue tuning. Hue representations thus remain highly robust along intensity-related dimensions, supporting stable color coding under dynamic illumination and environmental conditions. Moreover, luminance and saturation jointly modulate neural activity via gain mechanisms, providing physiological evidence that entopallium population activity supports stable hue-centered representations under varying luminance and saturation (Hanazawa et al., 2000).

Color representation of color-selective populations

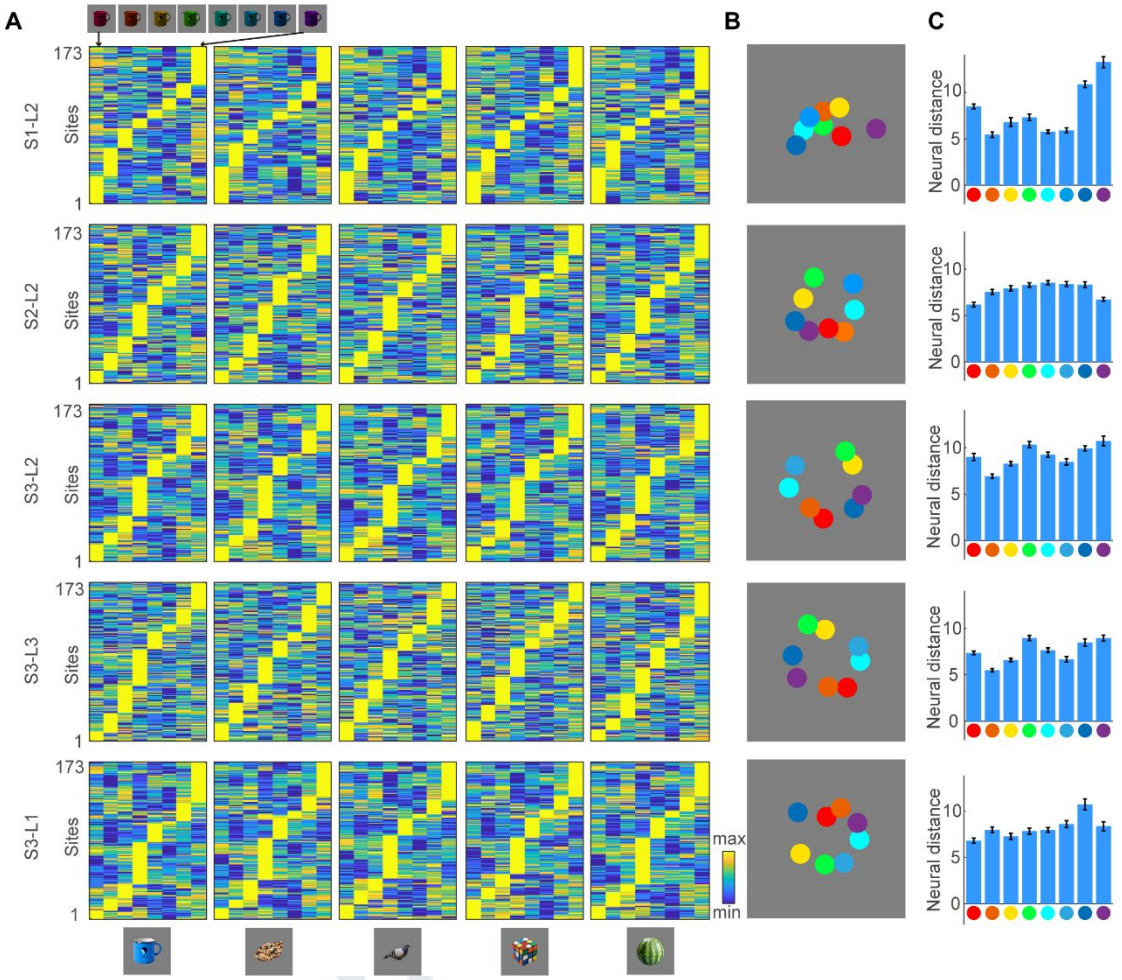

Figure 5 Color representation structure of color-selective populations

A: Neural response matrix showing the mean responses of all color-selective sites to 8 hues. Each column represents a object, and each row corresponds to one of 5 luminance-saturation. B: Color representation space: based on cross-object averaged neural responses, the 8 hues were projected into a 2-dimensional space using MDS. Gray dots denote the geometric center of each hue, illustrating the clustering structure and relative arrangement under different luminance-saturation. C: Neural distance between hues and gray: average neural distances between each hue and the gray stimulus, with error bars indicating standard deviations estimated from 20,000 bootstrap samples.

To further examine how luminance and saturation modulate the overall structure of color representation at the population level, we analyzed the response patterns of color-selective sites in Figure 5 (Conway and Stoughton, 2009; Schrader and Wachtler, 2023; Tanabe, 2013). Figure 5A shows population responses of color-selective sites to color stimuli, with sites

ordered by hue preference (rows) and hues by columns. Correlation analyses revealed strong cross-category consistency (mean similarity = 0.68) and moderate consistency across luminance-saturation conditions (0.44), indicating a stronger color tuning stability by categorical influence. Figure 5B shows hue representational spaces derived from averaged responses. Under low saturation (S1-L2), purple hues were overrepresented, whereas higher luminance and saturation (S3-L3) produced a more uniform, near-circular distribution resembling the CIE color space. Despite slight global deviations from CIE ordering, adjacent hue pairs (H1 and H2, H3 and H4, H5 and H6, H7 and H8) remained consistently close, indicating strong local continuity in hue representation. Figure 5C quantitatively evaluates hue arrangement in neural space. Under S1-L2, hue distances were uneven, with only a few hue pairs showing clear separation; in contrast, under S3-L3 conditions, hue distances became more uniform, indicating enhanced separability and isotropy of hue representations (Rosenthal et al., 2019).

Overall, the neural population in entopallium encoded hue consistently across object categories yet reconfigured with changes in luminance and saturation, yielding a more balanced and continuous inter-hue geometry. This pattern implies that color-selective entopallium sites preserve stable hue preferences across shape categories, while responses along intensity dimensions are modulated via gain modulation. Together, these findings delineate a dynamic stability-plasticity balance in avian color coding: robust hue representation is maintained alongside flexible adaptation to visual intensity. This advances understanding of color representation in the avian visual system and provides empirical support for organizational principles underlying multidimensional sensory integration.

Color and category representations of color-selective population

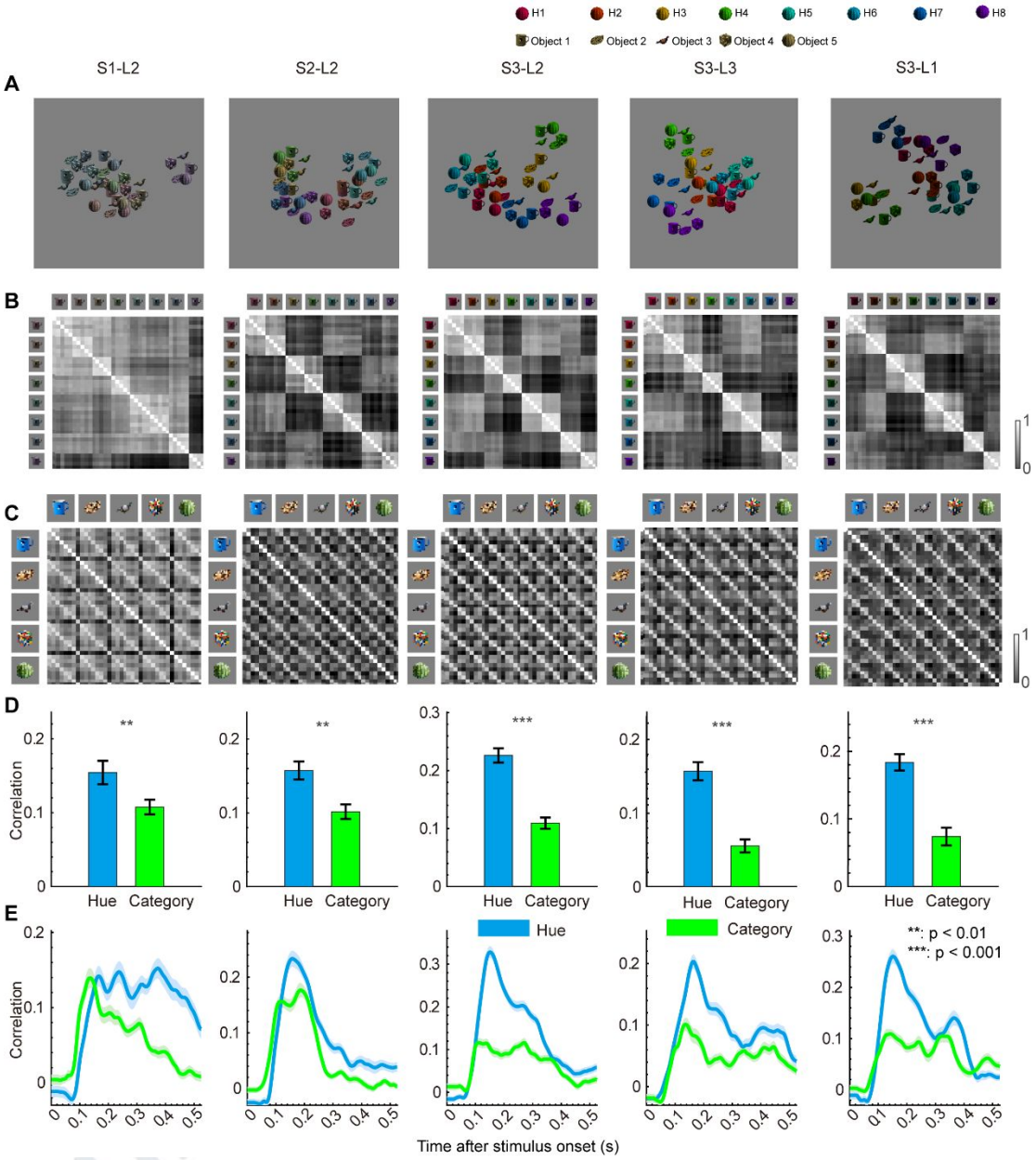

Figure 6 Comparative analysis of color and category representations in the color-selective population (n = 173 MUA sites)

A: MDS embeddings of population responses under each luminance–saturation (L-S) condition (S1-L2 to S3-L1). Each point represents one stimulus condition (5 objects × 8 hues) and is shown as an object icon (category) colored by its hue. Distances reflect dissimilarities between population response vectors (n = 173 MUA sites; averaged across repetitions), computed using Euclidean distance. Responses cluster primarily by hue; this hue-based grouping is less pronounced under S1-L2. Original stimulus images are omitted for visual clarity. B: Hue representational similarity matrix (RSM). Each matrix shows Pearson correlations (r) between population response vectors for the 40 stimuli (5 objects × 8 hues) under the corresponding L–S condition. Rows/columns are ordered by hue and then by object category. High similarity is observed for identical hues across different objects. C: Category

representational similarity matrix (RSM). Pearson correlations (r) were computed as in (b) for the same set of 40 stimuli, with rows/columns grouped by object category (blocks) and ordered by hue. Compared with the hue RSM, cross-category similarity is lower, indicating more distinct and less overlapping category representations in this color-selective population. D: Quantitative comparison of hue and category information. Mean within-category correlations across hues ("hue information") and within-hue correlations across categories ("category information") were computed. Error bars show standard deviations from 20,000 bootstrap samples. Across all conditions, hue information was significantly higher than category information (*: $p < 0.05$; **: $p < 0.01$; ***: $p < 0.001$). E. Temporal dynamics of representation. Mean correlation coefficients were calculated using a 50 ms sliding window within the first 500 ms after stimulus onset. The x-axis indicates time, the y-axis the mean correlation, and the shaded area shows standard deviations from 20,000 bootstrap samples.

To visualize the neural representational space of object color and category in the pigeon entopallium, we applied MDS to population responses across luminance-saturation conditions (Figure 6A). Each stimulus (hue × category) was projected into a two-dimensional space, where stimuli sharing the same hue clustered together regardless of category, indicating that hue forms the principal axis of color-selective representation. Under high saturation, hue clusters were more compact and well separated (silhouette = 0.623 for S3-L2; 0.665 for S3-L3), reflecting enhanced color discriminability. In contrast, low saturation yielded diffuse and overlapping clusters (silhouette = 0.446 for S1-L2), indicating weakened hue representation. With saturation fixed at S3, increasing luminance produced only a minor, nonsignificant rise in clustering strength, suggesting gain modulation rather than structural reorganization. Object categories did not form distinct clusters, reinforcing that hue is the dominant representational dimension in this population.

We further examined population response similarities across all hue-category combinations under different luminance conditions. Under high saturation (S3), responses to objects sharing the same hue exhibited a clearer and more distinct structure, reflecting enhanced discriminability and stability. In contrast, at lower luminance levels (S1, S2), matrix boundaries

became diffuse, and correlations between adjacent hues (e.g., H3 and H4, H5 and H6) remained high, indicating reduced separability and stronger local continuity (Figure 6B). Meanwhile, same-category correlations across hues remained low, suggesting that category coding is distributed rather than clustered, consistent with the MDS results (Figure 6C). Together, these findings demonstrate that hue provides a stable and continuous framework for color representation across objects and viewing conditions.

Within the color-selective population, we compared hue and category information to assess representational consistency. Hue information was significantly higher across all luminance-saturation conditions (paired t-test; Figure 6D), indicating more stable and selective responses. Time-resolved analysis (Figure 6E) showed a rapid rise in hue information 100-200ms after stimulus onset, peaking at 300-400ms, while category information remained lower. These results indicate that sites rapidly encode hue, establishing it as the dominant coding dimension (Azizi et al., 2019). At the population level, color representation in the entopallium is primarily organized along the hue axis. Hue representations remain stable across categories, while category information does not form distinct clusters. Luminance and saturation modulate representational geometry mainly through gain modulation: high values enhance hue separability and uniformity, making neural geometry resemble physical color space, whereas low saturation weakens it. Overall, these findings highlight the robustness and adaptive flexibility of hue coding in the entopallium. (Chang et al., 2017).

Neural decoding

To further assess the informational content of neural population activity in the pigeon entopallium during color encoding, we applied a supervised SVM classifier to decode color identity from neural responses evoked by color stimuli presented across multiple object shapes in Figure7. The experimental design followed a full factorial combination of eight hues and five object categories, enabling the decoding performance to reflect the stability of color discrimination across category contexts. The results revealed that the average decoding accuracy across the eight hues reached 65%, which was significantly above the theoretical chance level of 12.5%. Among these, hue H4 yielded the highest classification accuracy of 84.8%, indicating that entopallium population activity carries reliable and discriminable information about color identity as shown Figure 7A. Moreover, decoding accuracy increased steadily with the number of MUA sites included and plateaued at approximately 60-80 MUA sites, suggesting that color discrimination in the entopallium depends on a population-level cooperative coding mechanism rather than on independent single-site responses in Figure 7B.

This observation aligns with previous studies that have quantified the linearly decodable information content of neural populations using linear classifiers, supporting the notion that SVM decoding effectively captures the independent representational dimensions of color information in this region. In combination with representational similarity analyses, we further found that color-selective MUA sites in the entopallium maintained stable hue representations across variations in object shape, exhibiting pronounced category (shape) invariance. Collectively, these results demonstrate that color encoding in the entopallium is not only highly

discriminative and generalizable but also reflects an intermediate-level integration of color information, providing compelling evidence for the neural basis of color constancy in the avian visual system.

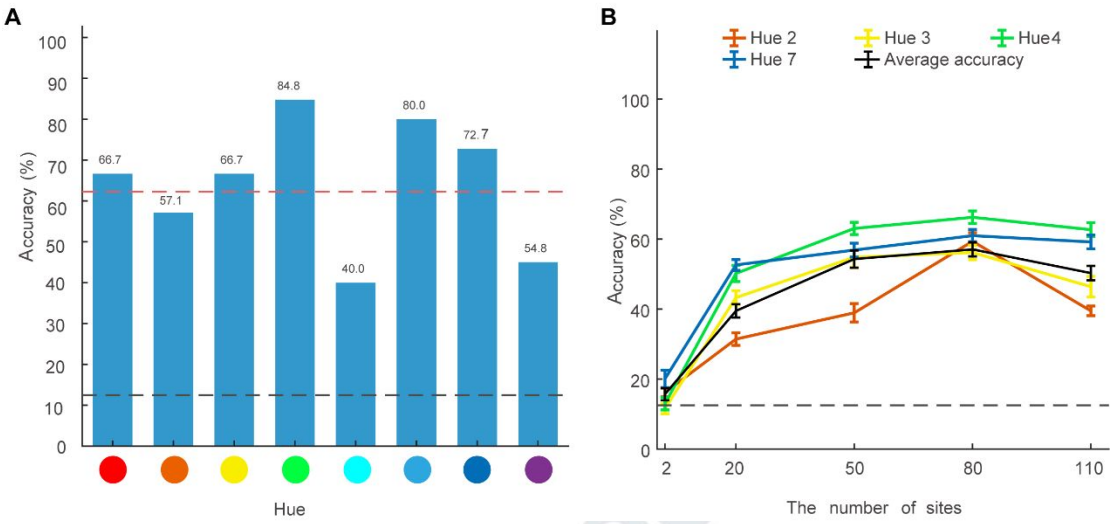

Figure 7 Decoding performance of color information in the color-selective population
A: SVM decoding accuracy. Classification accuracy for eight hues averaged across-object conditions. The black dashed line indicates the theoretical chance level (12.5%), and the red dashed line marks the mean decoding accuracy (≈65%). B: Population size and decoding performance. Effect of the number of MUA sites on classification accuracy, illustrating the cooperative nature of color encoding.

DISCUSSION

This study elucidates the neural representational characteristics of color-selective populations in the pigeon entopallium. Across luminance and saturation manipulations, signals recorded at MUA sites showed orderly hue tuning, with hue preferences remaining consistent across the tested object categories. Hue preferences are broadly and continuously distributed across the color space, forming an approximately uniform tuning pattern. At the population level, the representational geometry reorganizes globally with changes in luminance and saturation while preserving local hue relationships, reflecting a species-specific but

topologically stable coding scheme. Together, these findings show that the avian entopallium implements a robust and adaptive hue-centered architecture that maintains representational continuity under varying sensory conditions. Notably, across the tested conditions, color-related structure (and decoding) consistently exceeded category-related structure, indicating that entopallium population activity is more strongly organized by hue than by object category under the present stimulus set.

The stability of hue representation across luminance and saturation conditions observed in this study parallels findings from primate higher visual areas. In V4 and IT cortices, neurons preserve stable hue tuning across changes in luminance and saturation, while high-saturation stimuli markedly enhance population separability as well as decoding performance (Bichot et al., 2005; Conway and Tsao, 2009; Seymour et al., 2016; Zaidi and Conway, 2019). Likewise, the neural representations in entopallium remain structurally stable, with representational resolution scaling systematically with luminance and saturation—supporting a conserved computational principle whereby color constancy emerges through geometric continuity within representational space coupled with gain modulation. While excessive luminance differences can disrupt hue decoding in primates (Bohon et al., 2016; Brouwer and Heeger, 2009), the color-selective sites within the entopallium preserve coherent topological organization even under high-luminance/ high-saturation conditions, underscoring their structural resilience rather than geometric distortion. The “multidimensional feature co-tuning” identified in primate V4 and IT (Bohon et al., 2016; Lafer Sousa and Conway, 2013; Li et al., 2014) embodies a conserved computational principle across species, whereby hue, luminance, and saturation are jointly integrated through gain control to achieve stable neural encoding. Despite

pronounced anatomical divergence, avian and primate visual systems may converge on a conserved computational principle that supports perceptual constancy through color representations that are both stable and flexible.

Recent anatomical and imaging studies indicate that the avian brain, unlike the laminated primate neocortex, is organized into discrete nuclei with specialized functions (Briscoe and Ragsdale, 2018; Clark and Colombo, 2020; Stacho et al., 2020). Despite an early divergence in amniote evolution, birds and primates appear to have independently evolved effective color-guided behaviors under strong ecological pressures, including foraging and social signaling (Bennett and Théry, 2007; Osorio and Vorobyev, 2008). At the sensory periphery, avian color vision is supported by multiple cone photoreceptor classes, often including short-wavelength cones tuned to violet and, in some species, ultraviolet ranges, together with cone oil droplets that sharpen spectral tuning and enhance chromatic discrimination (Toomey et al., 2015). At the circuit level, the tectofugal pathway provides a major route to the forebrain and has been implicated in stimulus identification and chromatic processing, culminating in the entopallium. Comparative anatomical work has proposed parallels between avian pallial circuits and primate cortical processing streams, although direct functional equivalence remains unresolved (Stacho et al., 2020). Building on this comparative perspective, we used an orthogonal color and shape stimulus design to test how hue-related population structure in the entopallium is modulated by luminance and saturation. Our results support a role for the entopallium in population-level, multidimensional color representation under the tested conditions. We interpret the resemblance to primate V4 at the level of population representational geometry under comparable stimulus manipulations as reflecting shared computational tendencies for

organizing chromatic space, rather than evidence of structural homology or functional equivalence. Importantly, because the present study did not examine higher-order form processing or attentional modulation, which are strongly associated with primate V4, no conclusion can be drawn regarding whether the entopallium supports these broader integrative functions.

This study provides the systematic evidence populations of recording sites in the pigeon entopallium exhibit strong hue selectivity with minimal modulation by the tested object categories, consistent with category-invariant hue tuning. This finding advances our understanding of color processing in the avian visual system. While previous research in primates has established the V4 as central to color selectivity, hue invariance, and color constancy (Conway et al., 2007; Nigam et al., 2021; Tanigawa et al., 2010; Welbourne et al., 2023; Zeki, 1983), the neural basis of color selectivity in birds has remained largely unexplored despite behavioral evidence linking entopallium to color discrimination (Cook, 2013; Verhaal et al., 2012). Here, we show that entopallium MUA sites maintain consistent preferences for specific hues (e.g., red, green, blue) across object categories, a representational pattern consistent with stable chromatic coding under the tested conditions (Chang et al., 2017; Rosenthal et al., 2018; Wang et al., 2024). Using a comprehensive color-space design, we further demonstrate that entopallium sites exhibit continuous and broadly distributed hue tuning, reflecting a higher-order representational process that preserves stable color encoding across changes in object identity—positioning entopallium as a core region for color constancy and invariant object representation in the avian brain.

From an ecological perspective, the category-invariant hue structure observed here suggests that chromatic information can serve as a salient organizing dimension of entopallium population activity under the present stimulus set and recording approach (Scarf et al., 2016). In natural environments, color can convey behaviorally relevant information that generalizes across object identity and shape, including cues related to ripeness, social signaling, and learned discriminations The color representation that remains relatively tolerant to category variation could therefore promote stable and efficient use of color cues when object form is variable, degraded or partially occluded (Caves et al., 2018; Ham and Osorio, 2007). Importantly, whether the representational organization reported here confers measurable functional advantages in real-world tasks remains to be determined and will require direct behavioral validation. At the representational level, color-related representational structure and decoding performance in our data reliably exceeded category-related metrics, indicating that population activity is organized primarily along chromatic dimensions, whereas category information contributed comparatively less under the present stimulus set and recording approach. This population-level dominance of chromatic organization does not preclude category selectivity at the level of single neurons, but rather suggests that hue constitutes a principal axis of the recorded responses.

The physiological state of the animals should be considered when interpreting these results. Although urethane anesthesia supports stable recordings, it can alter response gain and the temporal dynamics of spiking relative to awake preparations. Moreover, our analyses are based on multi-unit activity at each recording site, which pools spikes from a small and potentially heterogeneous ensemble near the electrode contact (Buzsáki, 2004). As a result, the apparent

tuning at a site may reflect the activity of a dominant subset of units, mixtures of distinct subpopulations, or condition-dependent shifts in their relative contributions. Such pooling can make hue preferences appear more stable when contributing neurons share similar chromatic selectivity, while obscuring finer-scale mechanisms that require single-unit resolution. We therefore interpret our findings at the recording-site level, concluding that hue-related structure is robustly expressed in entopallium MUA and that local hue relationships within the representational geometry are preserved across luminance and saturation manipulations. Future studies using richer stimulus sets in awake, task-engaged animals, together with improved spike sorting or high-density recordings, will be important for linking these population-level signatures to underlying single-neuron diversity and circuit interactions under ethologically relevant conditions (Steinmetz et al., 2021).

Although the circuit basis of hue selectivity in the entopallium remains unresolved, the representational patterns observed here are consistent with convergent evolution of computational solutions for chromatic vision. The narrow hue tuning suggests that, along the avian visual pathway, chromatic information may be transformed from predominantly linear cone-opponent encoding at early thalamic relay stages, including the dorsolateral geniculate nucleus, into a more nonlinear and selective representation in the entopallium, mirroring hierarchical refinement in primate color processing (Bohon et al., 2016). The preservation of population-level structure across changes in luminance and saturation further indicates that robustness may be supported by neuronal heterogeneity, whereby neurons with diverse receptive-field profiles jointly encode chromatic information and attenuate the influence of input variability, a principle also advanced for macaque V4 (Nigam et al., 2021). From this

evolutionary perspective, these properties support the view that distantly related vertebrate lineages can converge on closely related population-coding strategies under shared ecological and physical constraints, including the requirement to maintain reliable chromatic signals despite substantial variation in illumination and contrast (Chang et al., 2017).

In conclusion, this study defines the organizational principles of color representation in the avian high-order visual system, revealing a striking functional similarity with primates in coding strategies. The entopallium exhibits stable hue tuning, category invariance, and adaptive modulation to physical color attributes. Together, these properties suggest that, despite the absence of a laminated cortical architecture, the avian brain achieves color constancy through geometric stability and gain modulation within its representation space. This finding refines our understanding of the functional organization of non-primate visual systems, indicating that color constancy may stem from an evolutionarily conserved computational principle—one that preserves geometric stability within high-dimensional representational space to maintain perceptual invariance. Collectively, these results uncover a distinct yet convergent neural strategy for color processing in birds, offering deeper insight into how visual systems evolve stable and efficient representations of sensory information.

CONCLUSION

Our findings demonstrate that the avian entopallium encodes color through stable hue tuning, category invariance, and adaptive gain modulation, forming a robust representational geometry. Despite lacking a layered cortex, birds achieve color constancy via a conserved computational strategy that stabilizes high-dimensional neural spaces. These results reveal a convergent

solution to color processing across birds and primates, underscoring shared organizational principles in visual system evolution.

DATA AVAILABILITY

The datasets used and analyzed in the current study are available from the corresponding author upon reasonable request. The raw data analyzed in this study are available from the Figshare (DOI: 10.6084/m9.figshare.30619316).

COMPETING INTERESTS

The authors declare that they have no competing interests.

AUTHORS' CONTRIBUTIONS

Q.Z.H. and J.C.Z. performed the experiments and composed the first draft. R.P.Z., B.L. and P.W. performed the experiments. X.K.N. and J.T.W. guided the experiments. Z.Z.W. polished and finalized the article and conceived and directed the project. All authors read and approved the final version of the manuscript.

ACKNOWLEDGMENTS

The authors gratefully acknowledge the teachers and students of the Military Engineering Platform, School of Electrical and Information Engineering, Zhengzhou University, for their valuable assistance and for kindly helping with the language refinement of the manuscript. This

work was funded by the National Natural Science Foundation of China (grant number: 62206253), and China Postdoctoral Science Foundation (grant number: 2024M752934).

REFERENCES

Azizi AH, Pusch R, Koenen C, Klatt S, Bröker F, Thiele S, et al. 2019. Emerging category representation in the visual forebrain hierarchy of pigeons (Columba livia). Behavioural Brain Research, 356: 423-434.

Bennett ATD, Cuthill IC. 1994. Ultraviolet vision in birds: What is its function? Vision Research, 34(11): 1471-1478.

Bennett Andrew tD, Théry M. 2007. Avian Color Vision and Coloration : Multidisciplinary Evolutionary Biology. The American Naturalist, 169: 1-6.

Bichot NP, Rossi AF, Desimone R. 2005. Parallel and serial neural mechanisms for visual search in macaque area V4. Science, 308(5721): 529 - 534.

Bohon KS, Hermann KL, Hansen T, Conway BR. 2016. Representation of perceptual color space in macaque posterior inferior temporal cortex (the V4 complex). eNeuro, 3(4): ENEURO.0039-0016.2016.

Bowmaker JK, Heath LA, Wilkie SE, Hunt DM. 1997. Visual pigments and oil droplets from six classes of photoreceptor in the retinas of birds. Vision Research, 37(16): 2183-2194.

Briscoe SD, Ragsdale CW. 2018. Homology, neocortex, and the evolution of developmental mechanisms. Science, 362(6411): 190 - 193.

Brouwer GJ, Heeger DJ. 2009. Decoding and reconstructing color from responses in human visual cortex. The Journal of Neuroscience, 29(44): 13992 - 14003.

Burley NT, Coopersmith CB. 2010. Bill color preferences of zebra finches. Ethology, 76(2): 133-151.

Buzsáki G. 2004. Large-scale recording of neuronal ensembles. Nature Neuroscience, 7(5): 446-451.

Caves E, Green P, Zipple M, Peters S, Johnsen S, Nowicki S. 2018. Categorical perception of colour signals in a songbird. Nature, 560(7718): 365-367.

Chang L, Bao P, Tsao DY. 2017. The representation of colored objects in macaque color patches. Nature Communications, 8(1): 2064.

Chen DM, Goldsmith TH. 1986. Four spectral classes of cone in the retinas of birds. Journal of Comparative Physiology A, 159(4): 473-479.

Clark W, Colombo M. 2020. The functional architecture, receptive field characteristics, and representation of objects in the visual network of the pigeon brain. Progress in Neurobiology, 195: 101781.

Collins SA, Hubbard C, Houtman AM. 1994. Female mate choice in the zebra finch — the effect of male beak colour and male song. Behavioral Ecology and Sociobiology, 35(1): 21-25.

Conway BR. 2009. Color vision, cones, and color-coding in the cortex. The Neuroscientist, 15(3): 274 - 290.

Conway BR, Moeller S, Tsao DY. 2007. Specialized color modules in macaque extrastriate cortex. Neuron, 56(3): 560-573.

Conway BR, Stoughton CM. 2009. Response: Towards a neural representation for unique hues. Current Biology, 19(11): R442-R443.

Conway BR, Tsao DY. 2009. Color-tuned neurons are spatially clustered according to color preference within alert macaque posterior inferior temporal cortex. Proceedings of the National Academy of Sciences, 106(42): 18034 - 18039.

Cook RG. 2013. Functional segregation of the entopallium in pigeons. Philosophy, 130(130): 59-86.

Endler JA, Westcott D, Madden JR, Robson TE. 2005. Animal visual systems and the evolution of color patterns: Sensory processing illuminates signal evolution. Evolution; international journal of organic evolution, 59(8): 1975-1818.

Ham AD, Osorio D. 2007. Colour preferences and colour vision in poultry chicks. Proc Biol Sci, 274(1621): 1941-1948.

Hanazawa A, Komatsu H, Murakami I. 2000. Neural selectivity for hue and saturation of colour in the primary visual cortex of the monkey. European Journal of Neuroscience, 12(5): 1753-1763.

Hart NS, Vorobyev M. 2005. Modelling oil droplet absorption spectra and spectral sensitivities of bird cone photoreceptors. Journal of Comparative Physiology A, 191(4): 381-392.

Haynes J-D. 2009. Decoding visual consciousness from human brain signals. Trends in Cognitive Sciences, 13(5): 194-202.

Hermann KL, Singh SR, Rosenthal IA, Pantazis D, Conway BR. 2022. Temporal dynamics of the neural representation of hue and luminance polarity. Nature Communications, 13(1): 661.

Hsiao YT, Chen TC, Yu PH, Huang DS, Hu F-R, Chuong CM, et al. 2020. Connectivity between nidopallium caudolateral and visual pathways in color perception of zebra finches. Scientific Reports, 10(1): 19382.

Hung CP, Kreiman G, Poggio T, Dicarlo JJ. 2005. Fast Readout of Object Identity from Macaque Inferior Temporal Cortex. Science, 310(5749): 863-866.

Jarvis ED, Güntürkün O, Bruce LL, Csillag A, Karten HJ, Kuenzel WJ, et al. 2005. Avian brains and a new understanding of vertebrate brain evolution. Nature Reviews Neuroscience, 6(2): 151-159.

Johnson EN, Hawken MJ, Shapley R. 2001. The spatial transformation of color in the primary visual cortex of the macaque monkey. Nature Neuroscience, 4(4): 409-416.

Kelber A. 2019. Bird colour vision – from cones to perception. Current Opinion in Behavioral Sciences, 30: 34-40.

Kelber A, Vorobyev M, Osorio DC. 2003. Animal colour vision — behavioural tests and physiological concepts. Biological Reviews, 78(1): 81-118.

Komatsu H, Ideura Y, Kaji S, Yamane S. 1992. Color selectivity of neurons in the inferior temporal cortex of the awake macaque monkey. Journal of Neuroscience, 12(2): 408-424.

Krützfeldt NO, Wild JM. 2005. Definition and novel connections of the entopallium in the pigeon (Columba livia). J Comp Neurol, 490(1): 40-56.

Lafer Sousa R, Conway BR. 2013. Parallel, multi-stage processing of colors, faces and shapes in macaque inferior temporal cortex. Nature Neuroscience, 16(12): 1870 - 1878.

Li M, Liu F, Juusola M, Tang S. 2014. Perceptual color map in macaque visual area V4. The Journal of Neuroscience, 34(1): 202 - 217.

Nigam S, Pojoga S, Dragoi V. 2021. A distinct population of heterogeneously color-tuned neurons in macaque visual cortex. Science Advances, 7(8): eabc5837.

Niu XK, Jiang ZY, Peng YY, Huang S, Wang ZZ, Shi LJaR. 2022. Visual cognition of birds

and its underlying neural mechanism: a review. Avian Research, 13: 100023.

Osorio D, Vorobyev M. 2008. A review of the evolution of animal colour vision and visual communication signals. Vision Research, 48(20): 2042-2051.

Price TD, Stoddard MC, Shevell SK, Bloch NI. 2019. Understanding how neural responses contribute to the diversity of avian colour vision. Animal Behaviour, 155: 297-305.

Pusch R, Clark W, Rose J, Güntürkün O. 2023. Visual categories and concepts in the avian brain. Animal Cognition, 26(1): 153-173.

Rosenthal IA, Hermann KL, Singh SR, Pantazis D, Conway BR. 2019. The geometry of color space uncovered by magnetoencephalography (MEG). Journal of Vision, 19(15): 4.

Rosenthal IA, Ratnasingam S, Haile T, Eastman S, Fuller-Deets J, Conway BR. 2018. Color statistics of objects, and color tuning of object cortex in macaque monkey. Journal of Vision, 18(11): 1.

Scarf D, Stuart M, Johnston M, Colombo M. 2016. Visual response properties of neurons in four areas of the avian pallium. J Comp Physiol A Neuroethol Sens Neural Behav Physiol, 202(3): 235-245.

Schrader F, Wachtler T. 2023. Hue-dependence of contextual influences in color vision explained by a non-uniform population code. Journal of Vision, 23(9): 5640.

Seymour KJ, Williams MA, Rich AN. 2016. The representation of color across the human visual cortex: Distinguishing chromatic signals contributing to object form versus surface color. Cerebral cortex, 26(5): 1997-2005.

Stacho M, Herold C, Rook N, Wagner H, Axer M, Amunts K, et al. 2020. A cortex-like canonical circuit in the avian forebrain. Science, 369(6511): eabc5534.

Stacho M, Ströckens F, Xiao Q, Güntürkün O. 2016. Functional organization of telencephalic visual association fields in pigeons. Behavioural Brain Research, 303: 93-102.

Steinmetz NA, Aydin C, Lebedeva A, Okun M, Pachitariu M, Bauza M, et al. 2021. Neuropixels 2.0: A miniaturized high-density probe for stable, long-term brain recordings. Science, 372(6539): eabf4588.

Stoughton CM, Conway BR. 2008. Neural basis for unique hues. Current Biology, 18(16): R698-R699.

Straight PJ, Gignac PM, Kuenzel WJ. 2024. Mapping the avian visual tectofugal pathway using 3D reconstruction. J Comp Neurol, 532(2): e25558.

Tanabe S. 2013. Population codes in the visual cortex. Neuroscience Research, 76(3): 101-105.

Tanigawa H, Lu HD, Roe AW. 2010. Functional organization for color and orientation in macaque V4. Nature Neuroscience, 13(12): 1542 - 1548.

Toomey MB, Collins AM, Frederiksen R, Cornwall MC, Timlin JA, Corbo JC. 2015. A complex carotenoid palette tunes avian colour vision. Journal of The Royal Society Interface, 12(111): 20150563.

Verhaal J, Kirsch JA, Vlachos IK, Manns M, Güntürkün O. 2012. Lateralized reward‐related visual discrimination in the avian entopallium. European Journal of Neuroscience, 35(8): 1337–1343.

Wang T, Lee TS, Yao H, Hong J, Li Y, Jiang H, et al. 2024. Large-scale calcium imaging reveals a systematic V4 map for encoding natural scenes. Nature Communications, 15(1): 6401.

Wang Z, Zhu J, Zhu M, He Q, Wu P, Niu X, et al. 2025. Multidimensional feature encoding and functional organization in the pigeon entopallium. Zoological Research:

10.24272/j.issn.22095-28137.22025.24217.

Watanabe S, Maier U, Bischof HJ. 2008. Pattern discrimination is affected by entopallial but not by hippocampal lesions in zebra finches. Behavioural Brain Research, 190(2): 201-205.

Welbourne LE, Martin JT, Segala FG, Wade AR, Baker DH. 2023. Contributed Session III: Measuring binocular combination of luminance and chromatic stimuli using fMRI. Journal of Vision, 23 (15): 83.

Xiao Q, Frost BJ. 2009. Looming responses of telencephalic neurons in the pigeon are modulated by optic flow. Brain Res, 1305: 40-46.

Xiao Y, Casti A, Xiao J, Kaplan E. 2007. Hue maps in primate striate cortex. NeuroImage, 35(2): 771-786.

Xiao Y, Wang Y, Felleman DJ. 2003. A spatially organized representation of colour in macaque cortical area V2. Nature, 421(6922): 535-539.

Zaidi Q, Conway BR. 2019. Steps towards neural decoding of colors. Current Opinion in Behavioral Sciences, 30: 169-177.

Zeigier HP, Bischoff H. 1994. Vision, brain, and behavior in birds. Optometry and Vision Science, 71: 641-643.

Zeki S. 1983. Colour coding in the cerebral cortex: The responses of wavelength-selective and colour-coded cells in monkey visual cortex to changes in wavelength composition. Neuroscience, 9(4): 767-781.